PCP
PLANT & CELL PHYSIOLOGY

Expression Patterns of Genes Encoding Sugar and Potassium Transport Proteins Are Simultaneously Upregulated or Downregulated When Carbon and Potassium Availability Is Modified in Shiraz (*Vitis vinifera* L.) Berries

Zelmari A. Coetzee[1,2,7,*], Rob R. Walker[2,3], Siyang Liao[2,4], Celia Barril[1,5], Alain J. Deloire[1,2,8], Simon J. Clarke[1,2], Stephen D. Tyerman[2,4] and Suzy Y. Rogiers[1,2,6]

[1]National Wine and Grape Industry Centre, Charles Sturt University, Locked Bag 588, Wagga Wagga 2678, Australia
[2]The Australian Research Council Training Centre for Innovative Wine Production, University of Adelaide, PMB 1, Glen Osmond, Adelaide 5064, Australia
[3]CSIRO Agriculture and Food, PMB 2, Glen Osmond, Adelaide 5064, Australia
[4]Australian Research Council Centre of Excellence in Plant Energy Biology, School of Agriculture, Food and Wine, Waite Research Institute, University of Adelaide, Glen Osmond 5064, Australia
[5]School of Agricultural and Wine Sciences, Charles Sturt University, Locked Bag 588, Wagga Wagga 2678, Australia
[6]NSW Department of Primary Industries, Wagga Wagga 2678, Australia
[7]Present address: Department of Jobs, Precincts and Regions, PO Box 905, Mildura, 3502, Australia.
[8]Present address: Montpellier SupAgro, 2 place Pierre Viala, Montpellier, 34060, France.
*Corresponding author: E-mail, zel.coetzee@agriculture.vic.gov.au; Fax, +61 467 407 279.
(Received October 12, 2018; Accepted June 27, 2019)

A link between the accumulation of sugar and potassium has previously been described for ripening grape berries. The functional basis of this link has, as of yet, not been elucidated but could potentially be associated with the integral role that potassium has in phloem transport. An experiment was conducted on Shiraz grapevines in a controlled environment. The accumulation of berry sugar was curtailed by reducing the leaf photoassimilation rate, and the availability of potassium was increased through soil fertilization. The study characterizes the relationship between the accumulation of sugar and potassium into the grape berry and describes how their accumulation patterns are related to the expression patterns of their transporter proteins. A strong connection was observed between the accumulation of sugar and potassium in the grape berry pericarp, irrespective of the treatment. The relative expression of proteins associated with sugar and potassium transport across the tonoplast and plasma membrane was closely correlated, suggesting transcriptional coregulation leading to the simultaneous translocation and storage of potassium and sugar in the grape berry cell.

Keywords: Gene expression • Grape berry pericarp • Potassium • Sugar • Transport proteins • *Vitis vinifera*.

Introduction

Speculation of a functional link between sugar and potassium (K^+) loading in the grape berry is based on the synchronous accumulation patterns of these two significant phloem mobile components during ripening (Deeken et al. 2002, Rogiers et al. 2006b). The underlying basis of the link is, although still unclear, likely associated with the role that K^+ plays in the long-distance transport of sugars from source to sink. Reasonable attention has been given to the loading mechanism of the phloem at the source in plant systems, but little research has addressed the unloading of photoassimilates, and the regulatory role of K^+ transport systems, in sink organs (Anschütz et al. 2014). A K^+ transporter, *AKT2/3*, detected in the phloem complex of the source and sink organs in *Arabidopsis* (Deeken et al. 2002), has been shown to regulate sucrose/H^+ symporters during active apoplastic phloem loading at the source (Pilot et al. 2003). In plants, sucrose is unloaded from the phloem at the sink by SUT1/SUC2 type transporters, similar symporters as for loading (Lemoine et al. 2013). It can therefore be speculated that a similar reverse mechanism to that of phloem loading may be operative in phloem unloading.

Grape berry growth follows a double sigmoidal curve with the two phases separated by a short lag phase (Hanana et al. 2007). The first phase is characterized by cell division followed by cell enlargement. The second phase begins with véraison (E-L 35; Dry and Coombe 2005), the viticultural term denoting the onset of ripening, and characterized by softening and coloration of the grape berries and the active accumulation of sugars.

Sugars are translocated from the source to the fruit by the phloem. A change from a symplastic to an apoplastic phloem unloading pathway, at the time when solutes start to actively accumulate in the sink, has been described by Zhang et al. (2006) in Kyoho grapes (*Vitis vinifera* × *Vitis labrusca* L.). This shift is common in many fruits (Hayes et al. 2007; Milne et al. 2018) and is necessary to overcome the high osmotic and hydrostatic pressure in the sink organs of fruit that load solutes in large quantities (Lalonde et al. 2003). K^+ is accumulated during both phases of berry growth and is delivered to the berry by the xylem and phloem (Çakir and Giachino 2012). After véraison, the contribution of K^+ from the xylem is

Plant Cell Physiol. 60(10): 2331–2342 (2019) doi:10.1093/pcp/pcz130, Advance Access publication on 10 July 2019, available online at https://academic.oup.com/pcp

thought to decline due to a surge in phloem flow (Afoufa-Bastien et al. 2010).

In grapevine, four sucrose transporter genes have been categorized and 59 putative hexose transporter genes, homologs to *Arabidopsis thaliana* proteins, have been identified by protein motif recognition (Manning et al. 2001, Afoufa-Bastien et al. 2010). *VvSUC12*, a member of the low-affinity SUCrose transporter group (SUT2/SUC3), was expressed at all developmental stages in the berry. Afoufa-Bastien et al. (2010) speculated that it is likely localized on the plasma membrane (**Fig. 1**) and involved in phloem unloading or the import of sucrose into berry cells. *VvHT3* (Hayes et al. 2007), a hexose transporter also known as *VvHT7* (Afoufa-Bastien et al. 2010), has not been functionally characterized, but this protein is also likely localized on the plasma membrane (**Fig. 1**) due to its similarity to *AtSTP7*. Three putative hexose–proton antiporters (*VvTMT1* to *VvTMT3*), classified as tonoplast monosaccharide transporters, have been identified in grapevine (Lecourieux et al. 2014). Afoufa-Bastien et al. (2010) construed that *VvHT6* is the same as *VvTMT1*.

Members of the SWEET sugar transporter family (Sugars Will Eventually be Exported Transporters) have been found to mediate the passive transport of sugars across membranes (Baker et al. 2012). *VvSWEET15* is a uniport sucrose efflux transporter from the SWEET family which is thought to be responsible for the unloading of sucrose into the leaf apoplast, the step prior to the loading of sucrose into the phloem complex (Chen et al. 2012). A reverse mechanism may thus exist in phloem unloading at the sink (Milne et al. 2018), with *VvSWEET15* mediating the passive unloading of sucrose into the apoplast of the berry (**Fig. 1**). *VvSWEET15* is highly expressed in the berry as indicated from transcriptomic datasets from different cultivars (Sweetman et al. 2012, Chong et al. 2014).

Even though grape berries are a strong sink for K^+, there is limited knowledge in relation to the transport mechanisms that drive its accumulation (Martins et al. 2012). The exception is work performed by Davies et al. (2006) who identified two K^+ UPtake transporters in the grape berry (*VvKUP1* and *VvKUP2*). Two inward rectifying K^+ channels localized on the plasma membrane, *VvK1.1* (Cuéllar et al. 2010) and *VvK1.2* (Cuéllar et al. 2013), have also since been described. Of note, Hanana et al. (2007) characterized a gene encoding a vacuolar cation/H^+ antiporter (*VvNHX1*) in the grape berry that likely facilitates vacuolar expansion (**Fig. 1**). The vital role that K^+ has in driving water entry into tissues (Marschner 2012) may thus also be relevant to the rapid berry growth that occurs with the onset of ripening. More recently Nieves-Cordones et al. (2019) characterized *VvK1.3*, an inward and outward weakly rectifying K^+ channel facilitating K^+ fluxes from the phloem to the berry apoplast.

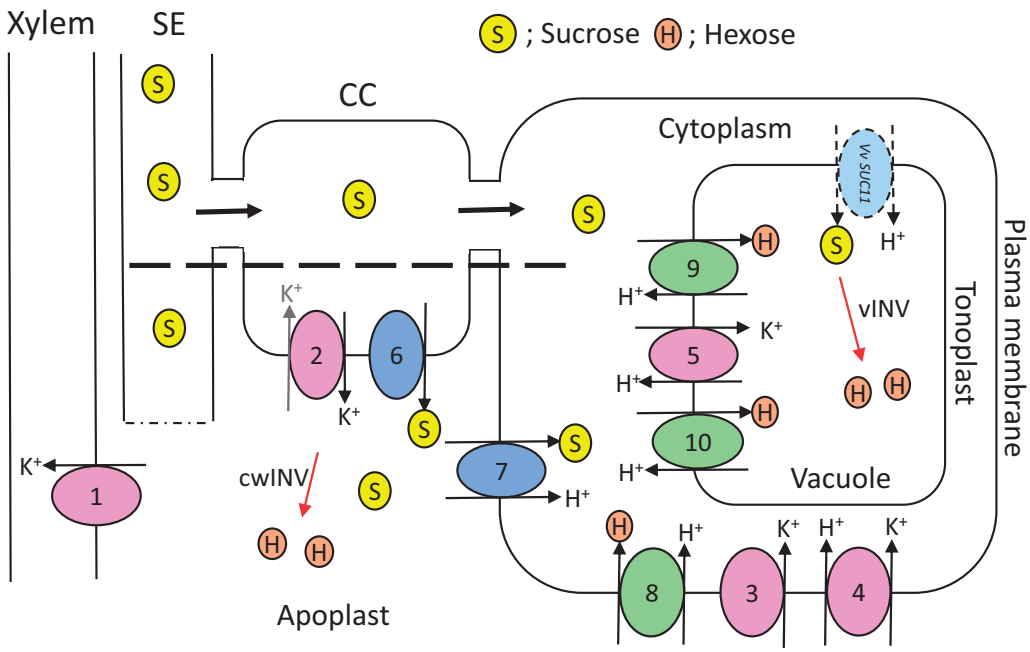

Fig. 1 Indication of the putative location of the assessed GOI associated with sucrose, hexose and K^+ transport in the grape berry. Five K^+ transport systems (pink) were assessed; three K^+ channels namely *VvSKOR* (1; Pilot et al. 2003), *VvKT2* (2; Deeken et al. 2002) and *VvK1.2* (3; Cuéllar et al. 2013), and a transporter *VvKUP2* (4; Davies et al. 2006). The tonoplast located *VvNHX1* K^+/H^+ antiporter (5; Hanana et al. 2007) is the only tonoplast K^+-transport system that has, to our knowledge, been identified in *V. vinifera*. Sucrose transporters (blue) shown are *VvSWEET15* (6; Chong et al. 2014) and *VvSUC12* (7; Afoufa-Bastien et al. 2010). A third sucrose transporter identified in the grape berry (*VvSUC11*; Manning et al. 2001) was not assessed in this study and the putative location is indicated with a broken border. Hexose transporters (green) included *VvHT3* (8; Hayes et al. 2007) and the two tonoplast hexose transporters *VvTMT1* (9; Afoufa-Bastien et al. 2010) and *VvTMT2* (10; Çakir and Giachino 2012). The demonstrated unloading pathways begin at the phloem sieve element (SE)—companion cell (CC) complex in the sink. The symplastic pathway is shown above and the apoplastic pathway below the broken line and arrows indicate the direction of movement of the solute. Sucrose molecules are shown as yellow circles and hexose sugar molecules, the product of sucrose hydrolysis by cell-wall invertase (cwINV) and vacuolar invertase (vINV), as orange circles.

Aquaporins are highly regulated during berry ripening and facilitate the movement of water, small molecules, gases and also ions under specific circumstances. They are part of the major intrinsic proteins superfamily and subdivided according to their subcellular location (Wong et al. 2018). Fouquet et al. (2008) identified nine genes encoding putative PIP (plasma membrane intrinsic proteins) and TIP (tonoplast intrinsic proteins) aquaporins in grape berries. *VvPIP2;1* was found to facilitate water and solute transport and strongly expressed during cell division and elongation.

In this study, we regulated the availability of sugar by altering the photoassimilation rate, and K^+ for loading into the ripening grape berry through modified fertilization. Genes that are known to code for proteins that mediate the transport of sugars and K^+ in the grape berry were identified and their kinetic expression patterns compared. The genes of interest (GOI) and their putative location are illustrated in **Fig. 1**. The objective was to define the relationship between the accumulation of sugar and K^+ in the grape berry as well as the potential coexpression of sugar and K^+ transporter protein genes during grape berry ripening.

Results

Berry development and ripening

The mean date of anthesis (flowering, E-L 23) for all vines was 28 d after budburst. Lowering the atmospheric CO_2 delayed the onset of ripening (véraison, E-L 35) from 63 ± 1 days after flowering (DAF) in the ambient CO_2 treatments to 66 ± 1 and 68 ± 2 DAF for the low CO_2 + standard K^+ and low CO_2 + increased K^+ treatments, respectively. At 101 DAF, the berries of both ambient CO_2 treatments were determined to be harvest ripe (E-L 38), and all treatments were harvested simultaneously.

The vines studied ($n = 48$) were comparable in mean leaf area, bunch mass and number of berries per bunch at the date of harvest (data not shown). Pericarp sugar, K^+ and water contents were similar between the treatments on the first sampling date (S1) prior to the start of the treatments (**Table 1**). There were also no differences ($P < 0.05$) in the sugar, K^+ and water content between treatments within a sampling date after treatments were started (S2–S7) due to the extensive variability in ripening between berries per replicate. The only exception was variation in the accumulation of water at S2 between the low CO_2 + standard K^+ and ambient CO_2 + increased K^+ treatment (**Table 1**).

The rapid accumulation of sugar occurred from véraison (S2) until S5 in all the treatments, increasing ≈1,140 and 1,300 µmol per berry pericarp from S2 to S5 in the low and ambient CO_2 treatments, respectively (**Table 1**). Although A_n was significantly reduced in the low CO_2 treatments (Supplementary Table S3), there were no differences in the pericarp sugar content between treatments (≈1,570 µmol sugar per pericarp) at harvest (S7) (**Table 1**). The accumulation rate of sugar decreased between S5 and S7 in all treatments. The decrease of ≈147 µmol in the mean pericarp sugar content of berries of the ambient CO_2 + standard K^+ treatment from S6 to S7, a decrease of ≈8%, was not statistically different at $P < 0.05$ (**Table 1**).

A tight curvilinear relationship was apparent between the mean pericarp sugar and K^+ contents across ripening (S1–S7), irrespective of treatment (**Fig. 2**) when assessed per biological replicate. High variability was, however, observed between the individual berries within a biological replicate (**Fig. 2**), even though véraison occurred at around the same time.

Gene expression patterns during berry ripening

For relative gene expression analyses, grape berry samples within a sampling date and treatment ($n = 12$ berries) were divided into three groups according to the date of véraison, resulting in three biological replicates ($n = 4$ berries per replicate) at three stages of ripening (early, mean and delayed ripening). The differences in berry ripeness are notable with large standard errors between biological replicates.

Prevéraison (S1) expression of *VvSWEET15*, responsible for the apoplastic unloading of sucrose from the companion cell, was discernibly variable in relation to the control, corresponding to the delay of véraison in the treatments (**Fig. 3**). Treatments, however, did not noticeably alter the expression of *VvSKOR* and *VvKT2* during ripening (S1–S6), with a similar trend apparent for *VvSUC12* (**Fig. 3**). Decreasing the atmospheric CO_2 did, however, increase the expression of *VvHT3*, a hexose transporter, from véraison (S2) onward (**Fig. 3**). A low atmospheric CO_2 concentration, combined with a standard application of K^+, increased the transport of K^+ across the plasma membrane following véraison as indicated by the greater expression of *VvKUP2* at S3, and *VvK1.2* at S3 and S4 (**Fig. 3**).

The treatments had a larger impact on the transcription of *VvTMT2* than *VvTMT1*, with a decrease in atmospheric CO_2 elevating the expression of *VvTMT2* postvéraison (S3 and S4), especially in combination with an increase in K^+ toward the end of ripening (S5 and S6) (**Fig. 3**). The increase in relative expression at S6 for *VvTMT2* was also evident in *VvPIP2;1* (**Fig. 3**).

Gene expression patterns at harvest

At harvest (S7), the relative expression of *VvK1.2*, *VvKUP2*, *VvTMT1* and *VvTMT2* increased in response to the reduced atmospheric CO_2 concentration (**Fig. 4**). The relative expression of *VvPIP2;1* was also elevated, with a 55-fold increase in the low CO_2 + increased K^+ treatment relative to the control (**Fig. 4**). In contrast, changes in the relative expression of *VvSKOR* were undiscernible due to the high relative expression of *VvSKOR* at harvest in the control treatment compared with the remainder of the treatments (**Fig. 4**; Supplementary Fig. S1). This increase in the expression of *VvSKOR* in the control treatment coincided with an increased expression of *VvBAG1* (**Fig. 5**).

Gene expression patterns of *VvBAG1* during berry ripening

VvBAG1 is a gene associated with programmed cell death in grape berries (S. Liao, personal communication) and was highly expressed in the control treatment (ambient CO_2 + standard

Table 1 Berry pericarp sugar, K^+ and water content per sampling date (S1 to S7) and per treatment

	Sampling date	Ambient CO_2 + standard K^+	Ambient CO_2 + increased K^+	Low CO_2 + standard K^+	Low CO_2 + increased K^+
Sugar content (μmol per pericarp)	S1	40 ± 11 d	55 ± 11 e	46 ± 23 d	43 ± 21 d
	S2	216 ± 88 d	306 ± 54 d	172 ± 84 d	202 ± 132 d
	S3	836 ± 36 c	766 ± 73 c	619 ± 192 c	514 ± 202 cd
	S4	1,336 ± 141 b	1,256 ± 28 b	1,063 ± 182 b	1,048 ± 266 bc
	S5	1,463 ± 117 ab	1,562 ± 108 a	1,347 ± 159 ab	1,307 ± 176 ab
	S6	1,712 ± 195 a	1,610 ± 106 a	1,506 ± 36 a	1,444 ± 220 ab
	S7	1,565 ± 159 ab	1,593 ± 106 a	1,510 ± 49 a	1,612 ± 153 a
K^+ content (μmol per pericarp)	S1	64 ± 3 e	70 ± 3 c	61 ± 3 c	61 ± 5 d
	S2	77 ± 6 de	88 ± 6 c	80 ± 6 bc	83 ± 3 cd
	S3	93 ± 5 cd	88 ± 6 c	80 ± 13 bc	74 ± 16 d
	S4	120 ± 13 bc	112 ± 3 b	112 ± 15 b	117 ± 17 bc
	S5	138 ± 6 ab	155 ± 10 a	150 ± 17 a	149 ± 9 ab
	S6	159 ± 14 a	143 ± 10 a	170 ± 5 a	168 ± 19 a
	S7	149 ± 12 a	152 ± 10 a	153 ± 5 a	174 ± 17 a
Water content (mmol per pericarp)	S1	47 ± 1 d	51 ± 2 d	48 ± 1 b	51 ± 4 c
	S2	56 ± 5 cd	62 ± 3 bc*	49 ± 3 b*	53 ± 3 bc
	S3	72 ± 1 ab	62 ± 4 bc	61 ± 6 a	61 ± 6 abc
	S4	74 ± 4 a	71 ± 2 ab	71 ± 4 a	73 ± 6 a
	S5	68 ± 3 ab	73 ± 4 a	68 ± 4 a	70 ± 3 a
	S6	76 ± 8 a	63 ± 2 abc	69 ± 3 a	69 ± 5 a
	S7	61 ± 4 bc	61 ± 3 c	63 ± 1 a	67 ± 6 ab

Data are presented as the mean of three biological replicates, representative of three ripeness levels, ±SE. Mean values assigned with different letters between sampling dates within treatments indicate significant differences ($P < 0.05$). No significant differences ($P < 0.05$) were observed between treatments within sampling dates and are not indicated, the only exception being the water content in S2, with treatments that differ indicated with an asterisk (*).

K^+) for the majority of the ripening period (Fig. 5). The prior application of high levels of K^+ fertilization decreased the expression of this gene toward harvest (S5–S7), relative to the standard K^+ application within both atmospheric treatments (Fig. 5). Decreasing the atmospheric CO_2 also inhibited the expression of the gene in relation to ambient CO_2 concentrations.

Interaction between the GOI, and the accumulation of sugar, K^+ and water in the grape berry

Hierarchical clustering analyses (Fig. 6) revealed that the clustering of the 11 GOI was relatively similar between the treatments, with similar upregulation and downregulation patterns between treatments which differed mainly in the extent of the regulation. The ambient CO_2 + increased K^+ treatment, however, behaved differently with the associations between the GOI changing within this treatment. *VvKT2* and *VvSKOR* were closely related independent of treatment, as well as *VvPIP2;1* with the two TMTs (Fig. 6). *VvK1.2* and *VvSWEET15*, both putatively associated with apoplastic transport, were related in three of the four treatments, with their relationship changing in the ambient CO_2 + increased K^+ treatment. Interesting to note is the close similarities in the expression patterns of *VvSUC12* and *VvNHX1*, independent of treatment. This association was extended to *VvHT3* in all treatments except for the ambient CO_2 + increased K^+ treatment where *VvHT3* was more closely related to *VvKUP2*.

Principal component analyses indicate a strong relationship between *VvNHX1* and *VvTMT1*, associated with the transport of K^+ and sugar, respectively, across the tonoplast (Fig. 7). K^+ falls in the same quadrant as these tonoplast transporters, signifying that *VvNHX1* may be responsible for K^+ loading in the vacuole to facilitate vacuolar expansion (Hanana et al. 2007). As in the hierarchical clustering, *VvK1.2* and *VvSWEET15* were closely associated, as were *VvKUP2* and *VvHT3*. *VvSKOR* and *VvKT2*, both transport proteins associated with the vascular system, were not closely associated with the remainder of the genes studied. *VvBAG1* was negatively related to transport proteins associated with transport across the tonoplast, as well as *VvHT3* and *VvKUP2*, suggesting a decrease in the transport into and the storage of sugar and K^+ within the grape berry cell vacuole as the expression of *VvBAG1* increases. The accumulation of sugar and water were tightly associated with the expression of the aquaporin transport protein *VvPIP2;1* (Fig. 7), which indicates that sugar loading in the grape berry cell is likely the main osmotic driver for the accumulation of water in the grape berry as previously suggested by Davies et al. (2006). Correlations between the GOI, and these GOI with the accumulation of sugar, K^+ and water, are shown for each treatment in Supplementary Table S1.

Discussion

This study was undertaken to characterize the kinetic expression patterns of characterized sugar and K^+ transport genes in ripening grape berries. A potential link in the accumulation of sugar and K^+ in grape berries has been alluded to in previous studies (Deeken et al. 2002, Rogiers et al. 2006b) after similar trends were observed in the accumulation patterns of these solutes during ripening.

Understanding the underlying mechanisms for the accumulation of K^+ in grape berries, in relation to that of sugar, is

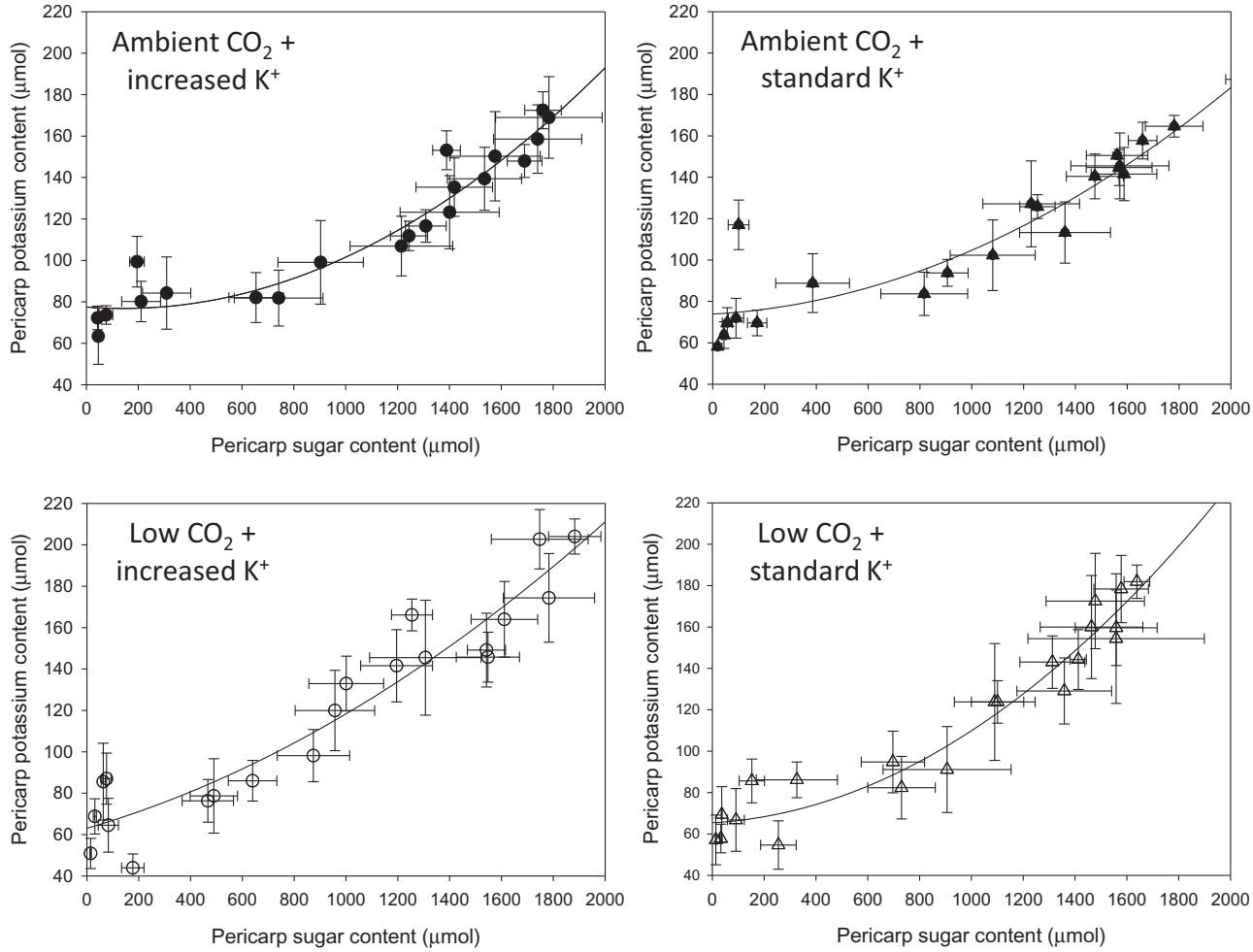

Fig. 2 The relationship between the K^+ and sugar (glucose and fructose) content of the berry pericarps separated by treatment with: $r = 0.93$, $P < 0.001$ for ambient CO_2 + increased K^+; $r = 0.92$, $P < 0.001$ for ambient CO_2 + standard K^+; $r = 0.95$, $P < 0.001$ for low CO_2 + increased K^+; and $r = 0.95$, $P < 0.001$ for low CO_2 + standard K^+. Triangles represent the standard K^+ and circles represent the increased K^+ fertilization treatments. Hollow symbols indicate the low CO_2 and solid symbols the ambient CO_2 atmospheric treatments. Values are the mean ± SE per biological replicate ($n = 4$ berries) across the complete ripening period ($n = 7$ sampling dates). Horizontal error bars represent the SE of the pericarp sugar content and vertical error bars the SE of the pericarp K^+ content.

challenging considering that K^+ plays a fundamental part in an array of plant functions (Cuéllar et al. 2013, Rogiers et al. 2017). K^+ is accumulated in the berry from fruit set (E-L 27) (Rogiers et al. 2006a), whereas sugar is only rapidly accrued from véraison (E-L 35) onward (Davies et al. 2012). The function and loading and unloading mechanisms of K^+ likely shifts at the onset of ripening, due to the osmotic changes resulting from the accumulation of large quantities of sugar and water in the berry, as well as the transition in phloem unloading from a symplastic to an apoplastic pathway (Zhang et al. 2006).

Accumulation of sugar, K^+ and water in the ripening grape berry pericarp

Photoassimilates, mainly sucrose in the grapevine (Keller 2010), are translocated from the sinks (leaves) to the source (grape berries) via the phloem and loaded in the grape berry cell through either a symplastic or apoplastic pathway (**Fig. 1**). In this study, the increased expression of transport systems associated with solute unloading into the apoplast and transport into the cell across the plasma membrane (**Fig. 1**) at around véraison (**Fig. 6**) supports the previously reported shift from symplastic to apoplastic phloem unloading at this developmental stage. The continuous removal of sucrose from the apoplast through the hydrolysis of sucrose by cell-wall invertase (cwINV) (Keller and Shrestha 2014) will sustain a downward sucrose gradient that will facilitate passive unloading of sucrose from the phloem complex, negating the need for an active phloem unloading pathway (Lecourieux et al. 2014).

The grape berry is a strong sink for photoassimilates during ripening (Lecourieux et al. 2014). Reducing the CO_2 in the atmosphere by 36% reduced photoassimilation by 35% (Supplementary Table S3). This reduced availability of sucrose did not, however, result in a decreased pericarp sugar content at harvest (**Table 1**). It is likely that carbohydrates were

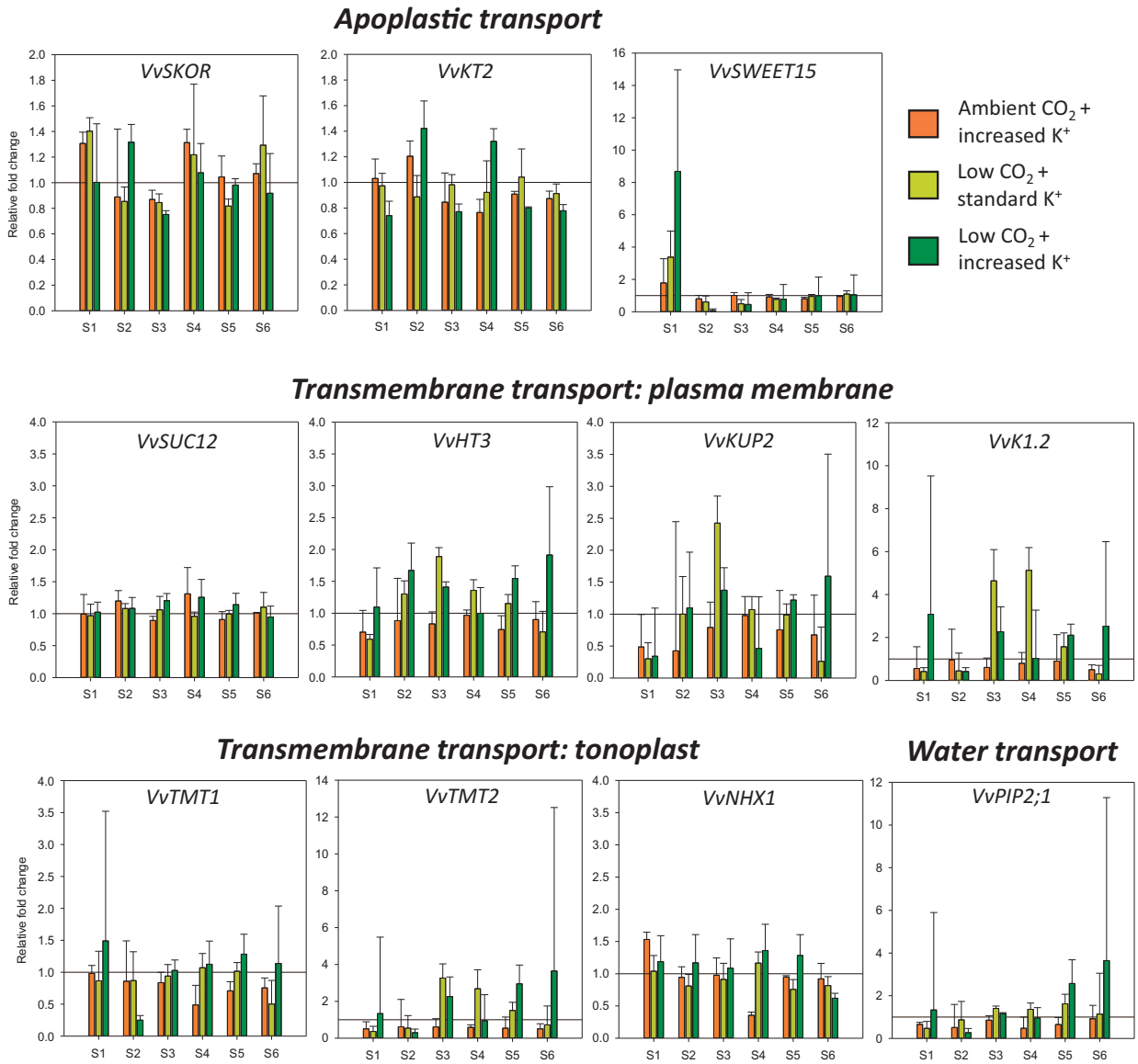

Fig. 3 The fold change in the expression of the GOI for the treatments relative to the control (ambient CO_2 + standard K^+) treatment and shown according to their putative transport pathway. Relative expression of the GOI were normalized against three reference genes (*VvActin7*, *VvEF1γ* and *VvGAPDH*). Expression data are presented for the ripening period (S1–S6) and values represent the mean of three biological replicates + SE.

remobilized from the perennial storage organs of the vine in the low CO_2 treatments to ensure optimal ripeness and guarantee seed dispersal. The remobilization of starch from the storage organs, more specifically the roots, under decreased photoassimilate availability has been described in previous studies (Candolfi-Vasconcelos et al. 1994, Rogiers et al. 2011, Coetzee et al. 2017, Rossouw et al. 2017).

Unlike the pericarp sugar content, the pericarp sugar concentration was 20% lower ($P < 0.05$) at harvest in the low CO_2 treatments and was accompanied with a higher percentage of water (data not shown). This could potentially be the result of the higher expression of *VvPIP2;1*, the most abundantly transcribed *PIP2* aquaporin isoform in grapevine (Choat et al. 2009, Tyerman et al. 2012), in the low CO_2 treatments toward the end of ripening (**Figs. 3**, **4**).

K^+ is accumulated in the berry prior to véraison and plays a large role in the prevéraison berry as an osmoticum to facilitate cell expansion (Davies et al. 2006). Similar to sugar, K^+ can enter the grape berry cell by either a symplastic or apoplastic pathway. *VvKT2* is associated with unloading of K^+ from the phloem (Ache et al. 2001) in the apoplastic space. The loading of K^+ from the apoplast to the cytoplasm is facilitated by *VvK1.2*, an inward rectifying K^+ channel (Cuéllar et al. 2013), and *VvKUP2*, a K^+ uptake transporter (Davies et al. 2006). *VvK1.2* is mainly associated with K^+ transport in the mesocarp cells (Cuéllar et al. 2013), whereas *VvKUP2* is predominantly expressed in the exocarp (skin) of the grape berry (Davies et al. 2006). The K^+ concentration of the skin is much higher than the mesocarp (Coombe 1987); thus a specialized molecular transport system, like *VvKUP2* which is able to actively

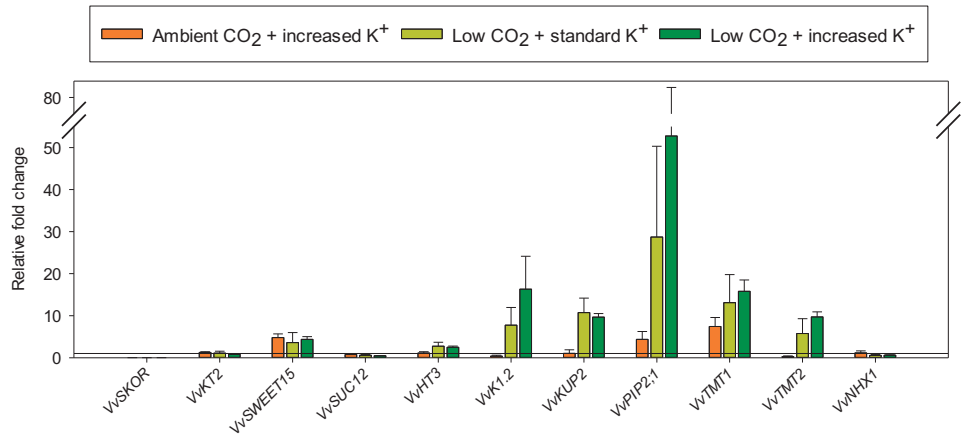

Fig. 4 The fold change in the expression of the GOI for the treatments relative to the control (ambient CO_2 + standard K^+) treatment at harvest (S7). Relative expression of the GOI were normalized against three reference genes (*VvActin7*, *VvEF1γ* and *VvGAPDH*) and values represent the mean of three biological replicates + SE.

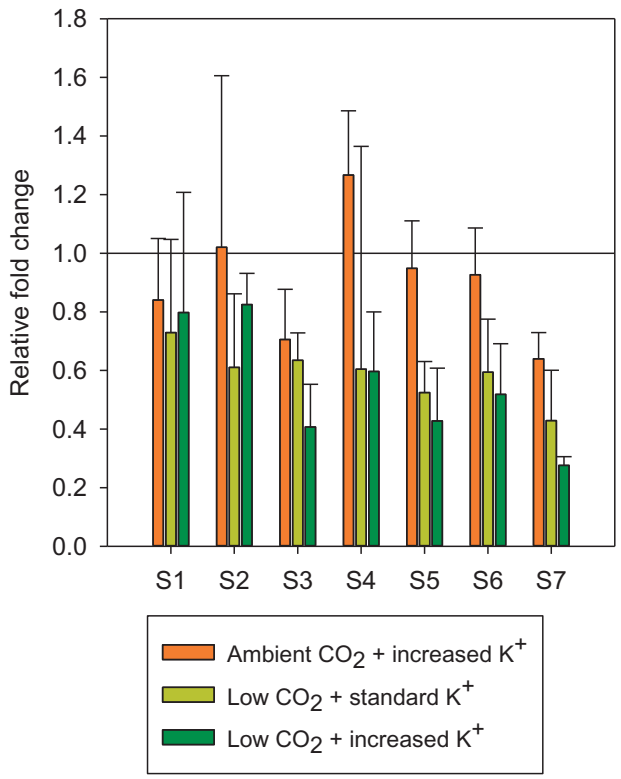

Fig. 5 The fold change in the expression of *VvBAG1* (S. Liao, unpublished work) for the treatments relative to the control (ambient CO_2 + standard K^+) treatment over the complete sampling period (S1–S7) with values representing the mean of three biological replicates + SE. Relative expression values were normalized against three reference genes (*VvActin7*, *VvEF1γ* and *VvGAPDH*).

transport K^+ across the plasma membrane against the concentration gradient, is needed to enable K^+ transport in the skin cells (Davies et al. 2006). A similar mechanism is needed in the mesocarp as the K^+ concentration of the cytoplasm is in general higher than that of the apoplast (Marschner 2012).

VvSKOR facilitates K^+ loading into the xylem of plant roots as an outwardly rectifying Shaker-like K^+ channel (Szczerba et al. 2009, Anschütz et al. 2014). The decrease in transcription of *VvSKOR* around véraison (**Fig. 6**; Supplementary Fig. S1) may be the result of decreased water and K^+ efflux from the xylem as the phloem pathway gains momentum and indicates potentially similar regulation in the grape berry to that in roots. It has by now been established that the xylem remains anatomically connected to the grape berry during ripening (Rogiers et al. 2000, Keller et al. 2006, Chatelet et al. 2008) and Tilbrook and Tyerman (2009) found that Shiraz berries had a larger tendency for backflow in the xylem than other cultivars. The continued transcription of *VvSKOR* during the postvéraison period (**Fig. 6**; Supplementary Fig. S1) could, therefore, be associated with the removal of excess water unloaded from the phloem, together with K^+, via backflow through the xylem as also proposed by Keller et al. (2006). *VvSKOR* activity is controlled by the K^+ concentration in the apoplast (Anschütz et al. 2014); thus, we can hypothesize that the efflux of water from the apoplast to the xylem would have increased K^+ concentrations and activated this channel. The decrease in berry water content at S7 (**Table 1**), pronounced in the ambient CO_2 + standard K^+ treatment, was thus likely due to a combination of a loss in water influx from the phloem, confirmed by the decreased expression of *VvPIP2;1*, and backflow through the xylem, potentially supported by the increased expression of *VvSKOR* (**Fig. 4**).

The increase in backflow through the xylem suggests a shift in the osmotic gradient due to an increased permeability of the plasma membrane. The increase in the transcription of the gene associated with cell death (*VvBAG1*) toward the end of ripening, specifically in the control treatment (**Fig. 5**), suggests an increase in apoptosis as ripening progressed in this study. With a loss of cell vitality, the berry cannot maintain a negative pressure between the pericarp apoplast and the xylem, and backflow may result (Tilbrook and Tyerman 2008, Tilbrook and Tyerman 2009).

Furthermore, the accumulation of reactive oxygen species (ROS), often associated with apoptosis, usually results in K^+

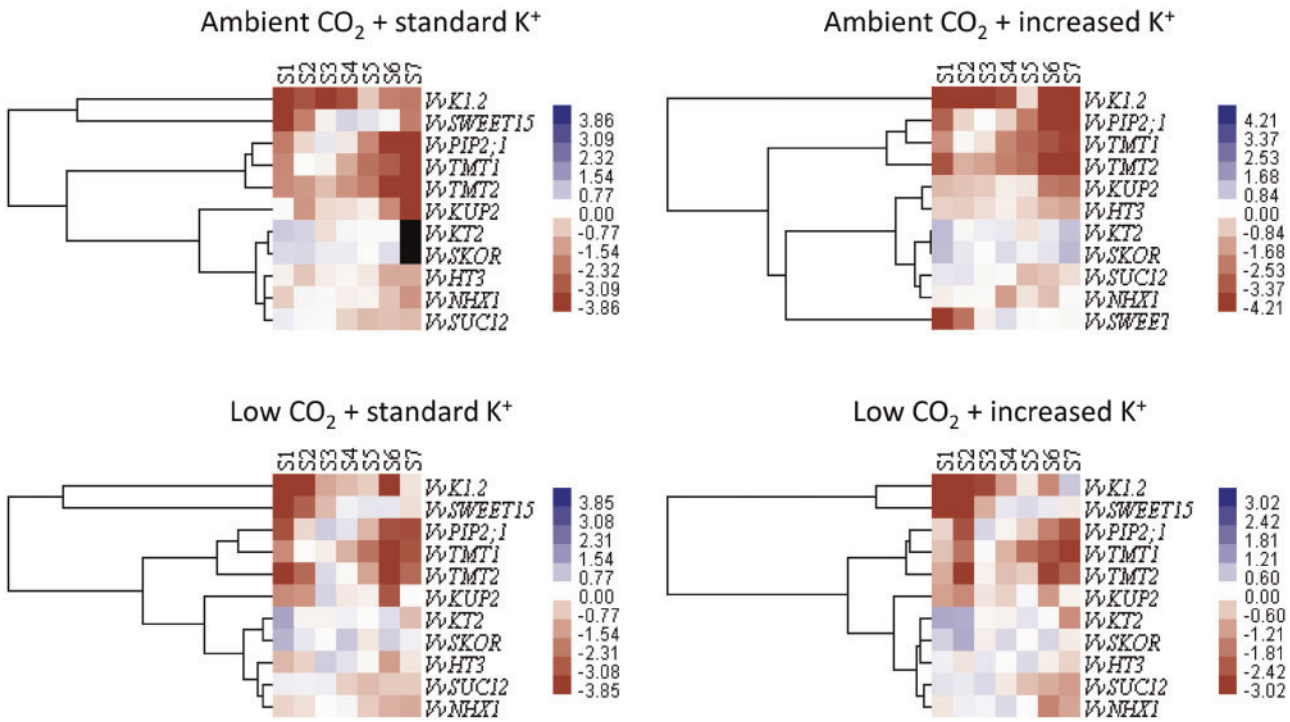

Fig. 6 Hierarchical cluster analyses of the relative expression data of the 11 GOI related to water, sugar and K^+ transport in the grape berry. The results of the expression levels are shown as a heatmap across the sampling dates and separated per treatment. Each row represents a GOI and each column a sampling date (S1–S7). The relative expression color scale per treatment represents the expression level per row.

efflux from plant cells under stress conditions. ROS contribute to K^+ leakage by activating outwardly rectifying K^+ channels, e.g. SKOR (stellar K^+ outward-rectifying channel) and also *AKT2*, a K^+-selective Shaker channel (Demidchik et al. 2014). A probable increase in ROS (not determined in this study) in the ambient CO_2 + standard K^+ treatment at S7, concomitant to the higher expression of *VvBAG1*, may explain the substantial increase in the expression of *VvSKOR* and *VvKT2* at harvest (Supplementary Fig. S1).

The change in the osmotic gradient brought on by the loss of cell vitality and permeability could also potentially explain the shifts in the accumulation patterns of sugar, water and K^+ as evident in the different treatments toward the end of ripening (**Table 1** and **Fig. 3**; Supplementary Fig. S1). The loss of membrane permeability, and the subsequent release of solutes from the cell into the apoplast, will hinder the functionality of e.g. *VvSWEET15* and *VvPIP2;1* as clearly evident in the control treatment at harvest (**Fig. 4**). The downregulation of *VvTMT1* and *VvTMT2* (**Fig. 4**), responsible for transporting hexose sugars across the tonoplast, indicates that less sugar was available for storage in the vacuole. The decrease in the pericarp sugar content at harvest in the control treatment pericarps (**Table 1**) is potentially the consequence of the cessation of sugar loading at the source in combination with cellular respiration.

Under controlled conditions, the transcription of *VvBAG1* was downregulated with an increase in K^+ fertilization (**Fig. 5**). Anschütz et al. (2014) noted that proteases and endonucleases are under strict control by K^+ and that a plant's ability to maintain cytosolic K^+ homeostasis impacts on stress-induced apoptosis. A loss of K^+ from plant cells will promote programmed cell death (Demidchik et al. 2014). Vines that received more K^+ during ripening were possibly able to relocate sufficient amounts of K^+ to the berry to sustain an optimal cytosolic K^+ concentration and thus able to curtail apoptosis. Further research will, however, be required to determine whether K^+ fertilization is able to suppress apoptosis in grape berries.

The relationship among the accumulation of sugar, K^+ and water in the berry pericarp

A solid correlation was apparent under controlled conditions between the pericarp sugar and K^+ content in this study (**Fig. 2**). Ten-fold more sugar molecules (glucose and fructose), however, accumulated by harvest (S7) in the berry in relation to the number of K^+ ions (**Table 1**).

The strongest evidence, to our knowledge, of the coregulation of K^+ and sugar transport was detected in the phloem complex of *Arabidopsis* during active phloem loading. Removal of H^+ from the apoplast as a consequence of the transport of sucrose and hexose sugars into the sink cell will activate the *VvKT2* channel, assuming that it behaves similarly to the *AKT2* channel in *Arabidopsis* (Ache et al. 2001). In grape berries, the relationship between sugar and K^+ loading is, hence, likely indirect and not the result of the coregulation of sugar unloading from the phloem by *VvKT2* as observed in other plant species.

Strong relationships observed in the relative expression levels between *VvKUP2* and *VvHT3*, *VvSWEET15* and *VvK1.2*,

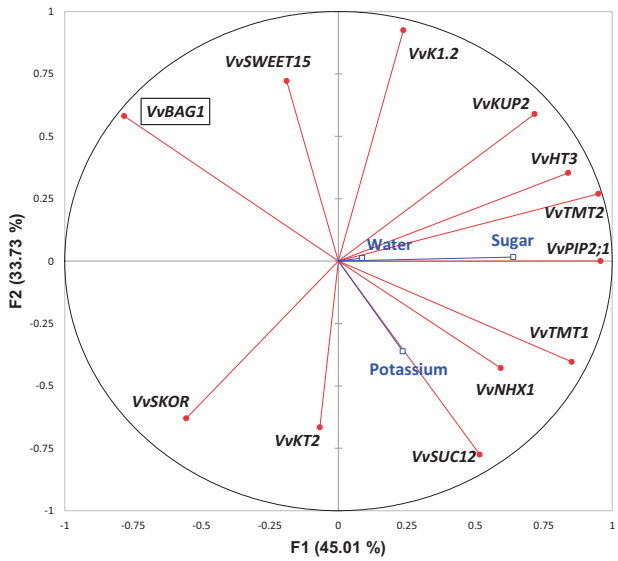

Fig. 7 Principal component analyses of the expression of the GOI associated with the transport of sugar, K^+ and water in the grape berry. Data represent all treatments for the complete sampling period (S1–S7). In addition, the relationship of *VvBAG1*, believed to be associated with berry cell apoptosis, is shown in relation to the transport proteins. F1 and F2 explain 78.74% of the variability observed in the data.

as well as *VvTMT1* and 2 with *VvNHX1* are indicative of potential link in the activation of transporters at every step of the berry loading pathway (**Fig. 6**). Water and sugar had a positive relationship with transporters that facilitate the transport of sugar and water across the cellular membrane and tonoplast (**Fig. 7**). The accumulation of K^+ was, however, mainly associated with the tonoplast transport systems (**Fig. 7**).

The relationship between the putative TMTs and *VvPIP2;1*, especially *VvTMT2* (**Figs. 6**, **7**), further alludes to the role of sugar as the main osmoticum after véraison. The close association between the expression of *VvPIP2;1* and the hexose and K^+ transport proteins putatively located on the tonoplast (**Figs. 6**, **7**) further alludes to a ternary linkage among the accumulation of sugar, K^+ and water in the grape berry. A ternary relationship among the accumulation of sugar, water and K^+ has previously been demonstrated in grape berries by Etchebarne et al. (2009) and Coetzee et al. (2017).

The large variability between and within the biological replicates, evident in both the content and transcription data (**Figs. 2**, **3**; Supplementary Fig. S1), however, highlights the plasticity in the accumulation of K^+ and sugar between grape berries. Gouthu et al. (2014) demonstrated that the transcription programs were dissimilar in grape berries located on the same bunch, but they also found that the rate of ripening increased in delayed berries during ripening, further indicative of plasticity in the ripening program. The continued expression of specific transporter proteins in the low CO_2 treatments associated with sugar, potassium and water transport into the grape berry pericarp at harvest (**Fig. 4**) might imply that the rate of ripening did not increase in the delayed ripening berries in this study. The effect of apoptosis on the expression of these transport proteins toward the end of ripening in the ambient CO_2 treatments should, however, not be ignored and may explain this disparity.

This study was undertaken to confirm the nexus between the accumulation of sugar and K^+ in the grape berry. In addition, we endeavored to ascertain if this relationship is based on the coregulation of sugar and K^+ transport systems.

Despite altering the relative availability of both solutes for transport to the grape berry, the link between the accumulation of sugar and K^+ into the pericarp was sustained. This relationship was also evident in the expression of transport proteins putatively located on the plasma membrane (*VvHT3* and *VvKUP2*) and sugar and K^+ transport across the tonoplast into the vacuole (*VvNHX1* and *VvTMT1*). The expression patterns of the GOI responsible for mediating sugar, K^+ and water transport across cell membranes were also closely correlated, which highlights the probability of a ternary linkage between them.

There is thus a strong indication that sugar, K^+ and likely water transport into the grape berry pericarp cells are coregulated, but there is variability in the strength of the regulation between berries. We, however, only assessed a small constituent of the transporter systems that are involved in water, sugar and K^+ transport in the grape berry cell, and only one cultivar under controlled conditions. The plasticity of grape berry ripening, not only between grape berries on a bunch and between vines but also between cultivars, necessitates further research on this topic in order to better understand the sugar-K^+ nexus in ripening fruit.

Materials and Methods

Plant material and growth conditions

Shiraz (*V. vinifera* L., clone SA1654) own-rooted vines were initially grown in bird-proof enclosures located at the National Wine and Grape Industry Centre, Australia (35°3′38.57″S; 147°21′42.89″E; 121 m). Vines were irrigated twice daily (3 l per vine per day) and hand fertilized every third day with a modified Hoagland's solution (Baby et al. 2014, solution 2). Phenological stages were visually determined according to the modified E-L system (Dry and Coombe 2005).

Forty-six DAF at E-L 33, vines were balanced by suckering each vine to one shoot yielding an archetypal bunch, topped at 21 leaves and the vines relocated to four controlled environment chambers ($n = 12$ vines per chamber) (TPG-6000-TH, Thermoline Scientific, Smithfield, Australia). The chambers were maintained at a 14-h photoperiod and 29.02 ± 0.02 and 20.87 ± 0.02°C day and night temperatures, respectively. The irrigation volume was reduced to 2 l per vine per day, ensuring that the vines were well watered without runoff through the bottom of the pot.

Environmental monitoring

Temperature and humidity were continuously monitored by TinyTag Plus 2 TGP-4500 dual channel dataloggers (Gemini dataloggers, West Sussex, UK) placed at mid-canopy height. The atmospheric CO_2 concentration was monitored at single time points by LCA-2 portable infrared carbon dioxide analyzers (ADC Bioscientific Ltd., Hoddesdon, Hertfordshire, UK) and continuously in alternating chambers by an LCA-4 portable infrared gas analyzer (IRGA) instrument (ADC Bioscientific Ltd.). The photon flux density was continuously monitored with Q-110 quantum sensors (Apogee Instruments Inc., Logan, UT, USA) connected to CR1000 data loggers (Campbell Scientific Inc., Logan, UT, USA). Soil moisture per vine was measured at single time points with an ML2x ThetaProbe soil moisture sensor connected to an HH2 moisture meter

(Delta-T Devices Ltd, Cambridge, UK). The environmental parameters are noted in Supplementary Table S2.

Leaf gas exchange

Leaf gas exchange measurements were conducted 52, 66, 73, 87 and 101 DAF on tagged leaves at the basal, median and apical positions of the shoot, and they and the data are shown in Supplementary Table S3. The net CO_2 assimilation rate (A_n), stomatal conductance (g_s), intercellular CO_2 concentration (C_i) and transpiration rate (E) were measured with an LI-6400 portable photosynthesis system (Li-Cor, Lincoln, NE, USA) at a leaf temperature of 28°C and a saturated light intensity of 1,200 μmol·m^{-2}·s^{-1}. The reference CO_2 concentration was set to 225 and 350 μmol CO_2·mol^{-1}, the mean atmospheric CO_2 concentration measured in the low and ambient CO_2 chambers, respectively.

Treatments and sample collection

Four treatment combinations were introduced 56 DAF just before the start of véraison (E-L 34). The atmospheric CO_2 concentration was reduced by 36% to ≈225 ppm in two chambers (low CO_2, L-treatment) by drawing the air within the chambers through sodalime filled (Sofnolime USP grade, Molecular Products Ltd, Essex, UK) custom-built scrubbers. The remaining two chambers were kept at ambient CO_2 levels (A-treatment). Fertilization of half the vines per chamber ($n = 6$) continued with the original modified Hoagland's solution (S-treatment), and the other half of the vines was fertilized with the original solution in which the K^+ concentration was increased by 67% to 12 mM (I-treatment). Four treatments were thus introduced: a low atmospheric CO_2, standard K^+ (LS) treatment; a low atmospheric CO_2, increased K^+ (LI) treatment; an ambient atmospheric CO_2, standard K^+ (AS) treatment; and an ambient atmospheric CO_2, increased K^+ (AI) treatment.

Berry samples were collected at 54, 61, 68, 75, 85, 94 and 103 DAF (presented as sampling dates S1–S7). Two berries per vine were harvested per sampling date by cutting randomly selected berries close to the pedicel. Berries were immediately flash frozen and stored at −80°C until further analyses. One berry per sample set was allocated for soluble sugars (glucose and fructose) and K^+ analyses and the second berry for gene expression analyses.

Berry pericarp soluble sugars and K^+ content analyses

The first set of berries, allocated for chemical analyses, was weighed frozen and the fresh mass noted. Each individual berry ($n = 336$) was then carefully separated into the seeds and pericarp (flesh and skin), ensuring the tissues remained frozen, the seed fresh mass determined and the pericarp fresh mass calculated.

Berry pericarps were thawed overnight at 4°C and individually ($n = 336$) homogenized (3 min at 20,000 rpm) with a handheld homogenizer (Benchmark D1000, Benchmark Scientific, Edison, NJ, USA). A 100-μl subsample of homogenized pericarp tissue was transferred to an Eppendorf tube with a positive displacement pipette (MICROMAN, Gilson Inc., Middleton, WI, USA) and the sample mass noted (Sartorius TE214S, Sartorius AG, Goettingen, Germany). Extraction and analyses of the glucose and fructose concentration per berry pericarp were performed by the method of Eyéghé-Bickong et al. (2012). Sugar values are shown as the sum of glucose and fructose. A further 50 μl of the homogenized pericarp tissue was transferred to a 3-ml borosilicate glass culture tube with a positive displacement pipette (MICROMAN, Gilson Inc.) and the sample mass noted (Sartorius TE214S, Sartorius AG). The samples were digested and the K^+ determined with flame atomic absorption spectrometry according to the method described by Coetzee et al. (2017).

Gene expression analyses

The second set of berries, allocated for gene expression analyses, was categorized within a sampling date into three biological replicates per treatment ($n = 4$ berries per replicate) according to the date of véraison (E-L 34) of the individual vines. The berry pericarps ($n = 84$ samples) were ground under liquid nitrogen, after removal of the seeds, to a fine powder with a mortar and pestle and stored at −80°C until further analyses.

RNA extraction and reverse transcription. Total RNA was isolated from ≈100 mg of ground pericarp tissue using a Spectrum Plant Total RNA Kit (Sigma-Aldrich, St. Louis, MO, USA) according to the manufacturer's guidelines. Remaining traces of DNA were removed with an On-Column DNase I Digestion Set (Sigma-Aldrich) during extraction as per the manufacturer's guidelines. A NanoDrop 1000 Spectrophotometer (ThermoFisher Scientific, Waltham, MA, USA) was used to determine the quantity and quality of the isolated RNA. First-strand cDNA was synthesized from 1 μg of total RNA with a SuperScript First-Strand Synthesis System for RT-PCR (Invitrogen, ThermoFisher Scientific) as prescribed in the manufacturer's guidelines.

Primers. GOI were selected from previously published work on the grounds that genes have been characterized in *V. vinifera* and have been found to be expressed in grape berries. Gene-specific primer pairs, specified in Supplementary Table S4, were designed with the use of Primer3 software and analyzed for dimerization with NetPrimer software (PREMIER Biosoft, Palo Alto, CA, USA). Primer pairs were checked for specificity with BLAST, and gel electrophoresis was used to check the dimerization of primer pairs and primer specificity validated from the amplicon size. The efficiency of each primer pair was tested through serial dilution of the PCR amplified product (One*Taq* Hot Start DNA Polymerase, New England BioLabs, Ipswich, MA, USA).

Comparative real-time quantitative polymerase chain reaction. Real-time quantitative polymerase chain reaction singleplex assays were performed on a QuantStudio 12K Flex Real-Time PCR System (Applied Biosystems, ThermoFisher Scientific). Biological replicate reactions were performed in triplicate on 20 μl volumes containing 10 μl PowerUp SYBR Green Master Mix (Applied Biosystems, ThermoFisher Scientific), 5 μl of a 1:10 dilution of cDNA template, 0.4 μl of each primer (10 μM) and 4.2 μl of nuclease-free water. Thermal cycles were: 2 min at 50°C, 2 min at 95°C and 40 cycles of 1 s at 95°C and 30 s at 60°C. Following the final cycle, specificity of the amplification was checked with a dissociation curve (15 s at 95°C, 1 min at 60°C and 15 s at 95°C). Gene transcript levels were normalized to three reference genes (*VvActin7*, *VvEF1γ* and *VvGAPDH*). Stability of the three reference genes was assessed with BestKeeper gene quantification software.

Statistical analyses

Statistical analyses were performed with Statistica 13 (StatSoft Inc., Dell Software, Round Rock, TX, USA) and XLSTAT 2013 (Addinsoft, Paris, France) statistical, and Sigmaplot 13 graphing (Systat Software Inc., San Jose, CA, USA) software. Relative quantification of the changes in gene expression compared with the untreated control was determined by the $2^{-\Delta\Delta CT}$ method (Livak and Schmittgen 2001). Hierarchical cluster analyses were performed with Cluster 3.0 software and visualized in Java TreeView. Berry accumulation data were combined as per the grouping of the berries per biological replicate prior to gene expression analyses. All values are presented as the mean of three biological replicates ± the standard error of the mean (SE) unless stated otherwise.

Supplementary Data

Supplementary data are available at PCP online.

Acknowledgments

The authors would like to thank the staff and students at the Australian Research Council Centre of Excellence in Plant Energy Biology [CE140100008] for their guidance during gene analyses.

Funding

The Australian Research Council Training Centre for Innovative Wine Production which is funded as a part of the Australian Research Council's Industrial Transformation Research Program [IC130100005] with support from Wine Australia and industry partners.

Disclosures

The authors have no conflicts of interest to declare.

References

Ache, P., Becker, D., Deeken, R., Dreyer, I., Weber, H. and Fromm, J. (2001) VFK1, a *Vicia faba* K^+ channel involved in phloem unloading. *Plant J.* 27: 571–580.

Afoufa-Bastien, D., Medici, A., Jeauffre, J., Coutos-Thevenot, P., Lemoine, R. and Atanassova, R. (2010) The *Vitis vinifera* sugar transporter gene family: phylogenetic overview and macroarray expression profiling. *BMC Plant Biol.* 10: 245.

Anschütz, U., Becker, D. and Shabala, S. (2014) Going beyond nutrition: regulation of potassium homoeostasis as a common denominator of plant adaptive responses to environment. *J. Plant Physiol.* 171: 670–687.

Baby, T., Hocking, B., Tyerman, S.D., Gilliham, M. and Collins, C. (2014) Modified method for producing grapevine plants in controlled environments. *Am. J. Enol. Vitic.* 65: 261–267.

Baker, R.F., Leach, K.A. and Braun, D.M. (2012) SWEET as sugar: new sucrose effluxers in plants. *Mol. Plant* 5: 766–768.

Çakir, B. and Giachino, R.R.A. (2012) VvTMT2 encodes a putative tonoplast monosaccharide transporter expressed during grape berry (*Vitis vinifera* cv. Sultanine) ripening. *Plant Omics* 5: 576–583.

Candolfi-Vasconcelos, M.C., Candolfi, M.P. and Kohlet, W. (1994) Retranslocation of carbon reserves from the woody storage tissues into the fruit as a response to defoliation stress during the ripening period in *Vitis vinifera* L. *Planta* 192: 567–573.

Chatelet, D.S., Rost, T.L., Shackel, K.A. and Matthews, M.A. (2008) The peripheral xylem of grapevine (*Vitis vinifera*). 1. Structural integrity in post-véraison berries. *J. Exp. Bot.* 59: 1987–1996.

Chen, L.-Q., Qu, X.-Q., Hou, B.-H., Sosso, D., Osorio, S., Fernie, A.R., et al. (2012) Sucrose efflux mediated by SWEET proteins as a key step for phloem transport. *Science* 335: 207–211.

Choat, B., Gambetta, G.A., Shackel, K.A. and Matthews, M.A. (2009) Vascular function in grape berries across development and its relevance to apparent hydraulic isolation. *Plant Physiol.* 151: 1677–1687.

Chong, J., Piron, M.-C., Meyer, S., Merdinoglu, D., Bertsch, C. and Mestre, P. (2014) The SWEET family of sugar transporters in grapevine: VvSWEET4 is involved in the interaction with *Botrytis cinerea*. *J. Exp. Bot.* 65: 6589–6601.

Coetzee, Z.A., Walker, R.R., Deloire, A.J., Barril, C., Clarke, S.J. and Rogiers, S.Y. (2017) Impact of reduced atmospheric CO_2 and varied potassium supply on carbohydrate and potassium distribution in grapevine and grape berries (Vitis vinifera L.). *Plant Physiol. Biochem.* 120: 252–260.

Coombe, B.G. (1987) Distribution of solutes within the developing grape berry in relation to its morphology. *Am. J. Enol. Vitic.* 38: 120–127.

Cuéllar, T., Azeem, F., Andrianteranagna, M., Pascaud, F., Verdeil, J.-L., Sentenac, H., et al. (2013) Potassium transport in developing fleshy fruits: the grapevine inward K^+ channel VvK1.2 is activated by CIPK–CBL complexes and induced in ripening berry flesh cells. *Plant J.* 73: 1006–1018.

Cuéllar, T., Pascaud, F., Verdeil, J.-L., Torregrosa, L., Adam-Blondon, A.-F., Thibaud, J.-B., et al. (2010) A grapevine Shaker inward K^+ channel activated by the calcineurin B-like calcium sensor 1–protein kinase CIPK23 network is expressed in grape berries under drought stress conditions. *Plant J.* 61: 58–69.

Davies, C., Boss, P.K., Gerós, H., Lecourieux, F. and Delrot, S. (2012) Source/sink relationships and molecular biology of sugar accumulation in grape berries. *In* The Biochemistry of the Grape Berry. Edited by Chaves, M., Gerós, H. and Delrot, S. pp. 44–66. Bentham Science Publishers, Sharjah.

Davies, C., Shin, R., Liu, W., Thomas, M.R. and Schachtman, D.P. (2006) Transporters expressed during grape berry (*Vitis vinifera* L.) development are associated with an increase in berry size and berry potassium accumulation. *J. Exp. Bot.* 57: 3209–3216.

Deeken, R., Geiger, D., Fromm, J., Koroleva, O., Ache, P., Langenfeld-Heyser, R., et al. (2002) Loss of the AKT2/3 potassium channel affects sugar loading into the phloem of *Arabidopsis*. *Planta* 216: 334–344.

Demidchik, V., Straltsova, D., Medvedev, S.S., Pozhvanov, G.A., Sokolik, A. and Yurin, V. (2014) Stress-induced electrolyte leakage: the role of K^+-permeable channels and involvement in programmed cell death and metabolic adjustment. *J. Exp. Bot.* 65: 1259–1270.

Dry, P.R. and Coombe, B.G. (2005) Viticulture. Volume 1, Resources. Winetitles, Adelaide.

Etchebarne, F., Ojeda, H. and Deloire, A. (2009) Influence of water status on mineral composition of berries in 'Grenache Noir' (*Vitis vinifera* L.). *Vitis* 48: 63–68.

Eyéghé-Bickong, H.A., Alexandersson, E.O., Gouws, L.M., Young, P.R. and Vivier, M.A. (2012) Optimisation of an HPLC method for the simultaneous quantification of the major sugars and organic acids in grapevine berries. *J. Chromatogr. B Analyt. Technol. Biomed. Life Sci.* 885–886: 43–49.

Fouquet, R., Léon, C., Ollat, N. and Barrieu, F. (2008) Identification of grapevine aquaporins and expression analysis in developing berries. *Plant Cell Rep.* 27: 1541–1550.

Gouthu, S., O'Neil, S.T., Di, Y., Ansarolia, M., Megraw, M. and Deluc, L.G. (2014) A comparative study of ripening among berries of the grape cluster reveals an altered transcriptional programme and enhanced ripening rate in delayed berries. *J. Exp. Bot.* 65: 5889–5902.

Hanana, M., Cagnac, O., Yamaguchi, T., Hamdi, S., Ghorbel, A. and Blumwald, E. (2007) A grape berry (*Vitis vinifera* L.) cation/proton antiporter is associated with berry ripening. *Plant Cell Physiol.* 48: 804–811.

Hayes, M.A., Davies, C. and Dry, I.B. (2007) Isolation, functional characterization, and expression analysis of grapevine (*Vitis vinifera* L.) hexose transporters: differential roles in sink and source tissues. *J. Exp. Bot.* 58: 1985–1997.

Keller, M. (2010) The Science of Grapevines: Anatomy and Physiology. Elsevier Science, Burlington.

Keller, M. and Shrestha, P.M. (2014) Solute accumulation differs in the vacuoles and apoplast of ripening grape berries. *Planta* 239: 633–642.

Keller, M., Smith, J.P. and Bondada, B.R. (2006) Ripening grape berries remain hydraulically connected to the shoot. *J. Exp. Bot.* 57: 2577–2587.

Lalonde, S., Tegeder, M., Throne-Holst, M., Frommer, W.B. and Patrick, J.W. (2003) Phloem loading and unloading of sugars and amino acids. *Plant, Cell Environ* 26: 37–56.

Lecourieux, F., Kappel, C., Lecourieux, D., Serrano, A., Torres, E., Arce-Johnson, P., et al. (2014) An update on sugar transport and signalling in grapevine. *J. Exp. Bot.* 65: 821–832.

Lemoine, R., La Camera, S., Atanassova, R., Dédaldéchamp, F., Allario, T., Pourtau, N., et al. (2013) Source to sink transport and regulation by environmental factors. *Front. Plant Sci.* 4: 1–21.

Livak, K.J. and Schmittgen, T.D. (2001) Analysis of relative gene expression data using real-time quantitative PCR and the $2^{-\Delta\Delta CT}$ method. *Methods* 25: 402–408.

Manning, K., Davies, C., Bowen, H.C. and White, P.J. (2001) Functional characterization of two ripening-related sucrose transporters from grape berries. *Ann. Bot.* 87: 125–129.

Marschner, H. (2012) Marschner's Mineral Nutrition of Higher Plants. Academic Press, London, UK.

Martins, V., Cunha, A., Gerós, H., Hanana, M. and Blumwald, E. (2012) Mineral compounds in the grape berry. *In* The Biochemistry of the Grape Berry. Edited by Gerós, H., Chaves, M.M. and Delrot, S. pp. 23–43. Bentham Science Publishers, Sharjah.

Milne, R.J., Grof, C.P.L. and Patrick, J.W. (2018) Mechanisms of phloem unloading: shaped by cellular pathways, their conductances and sink function. *Curr. Opin. Plant Biol.* 43: 8–15.

Nieves-Cordones, M., Andrianteranagna, M., Cuéllar, T., Chérel, I., Gibrat, R., Boeglin, M., et al. (2019) Characterization of the grapevine Shaker K^+ channel VvK3.1 supports its function in massive potassium fluxes necessary for berry potassium loading and pulvinus-actuated leaf movements. *New Phytol.* 222: 286–300.

Pilot, G., Gaymard, F., Mouline, K., Chérel, I. and Sentenac, H. (2003) Regulated expression of *Arabidopsis* Shaker K^+ channel genes involved in K^+ uptake and distribution in the plant. *Plant Mol. Biol.* 51: 773–787.

Rogiers, S.Y., Coetzee, Z.A., Walker, R.R., Deloire, A. and Tyerman, S.D. (2017) Potassium in the grape (*Vitis vinifera* L.) berry: transport and function. *Front. Plant Sci.* 8: 1629.

Rogiers, S.Y., Greer, D.H., Hatfield, J.M., Orchard, B.A. and Keller, M. (2006a) Mineral sinks within ripening grape berries (*Vitis vinifera* L.). *Vitis* 45: 115–123.

Rogiers, S.Y., Greer, D.H., Hatfield, J.M., Orchard, B.A. and Keller, M. (2006b) Solute transport into Shiraz berries during development and late-ripening shrinkage. *Am. J. Enol. Vitic.* 57: 73–80.

Rogiers, S.Y., Keller, M., Holzapfel, B.P. and Virgona, J.M. (2000) Accumulation of potassium and calcium by ripening berries on field vines of *Vitis vinifera* (L) cv. Shiraz. *Aust. J. Grape Wine Res.* 6: 240–243.

Rogiers, S.Y., Smith, J.P., Holzapfel, B.P. and Hardie, W.J. (2011) Soil temperature moderates grapevine carbohydrate reserves after bud break and conditions fruit set responses to photoassimilatory stress. *Funct. Plant Biol.* 38: 899–909.

Rossouw, G.C., Smith, J.P., Barril, C., Deloire, A. and Holzapfel, B.P. (2017) Carbohydrate distribution during berry ripening of potted grapevines: impact of water availability and leaf-to-fruit ratio. *Sci. Hortic.* 216: 215–225.

Sweetman, C., Wong, D.C., Ford, C.M. and Drew, D.P. (2012) Transcriptome analysis at four developmental stages of grape berry (*Vitis vinifera* cv. Shiraz) provides insights into regulated and coordinated gene expression. *BMC Genomics* 13: 691.

Szczerba, M.W., Britto, D.T. and Kronzucker, H.J. (2009) K^+ transport in plants: physiology and molecular biology. *J. Plant Physiol.* 166: 447–466.

Tilbrook, J. and Tyerman, S.D. (2008) Cell death in grape berries: varietal differences linked to xylem pressure and berry weight loss. *Funct. Plant Biol.* 35: 173–184.

Tilbrook, J. and Tyerman, S.D. (2009) Hydraulic connection of grape berries to the vine: varietal differences in water conductance into and out of berries, and potential for backflow. *Funct. Plant Biol.* 36: 541–550.

Tyerman, S.D., Chaves, M.M. and Barrieu, F. (2012) Water relations of the grape berry and aquaporins. *In* The Biochemistry of the Grape Berry. Edited by Gerós, H., Chaves, M.M. and Delrot, S. pp. 3–22. Bentham Science Publishers, Sharjah.

Wong, D.C.J., Zhang, L., Merlin, I., Castellarin, S.D. and Gambetta, G.A. (2018) Structure and transcriptional regulation of the major intrinsic protein gene family in grapevine. *BMC Genomics* 19: 248.

Zhang, X.-Y., Wang, X.-L., Wang, X.-F., Xia, G.-H., Pan, Q.-H., Fan, R.-C., et al. (2006) A shift of phloem unloading from symplasmic to apoplasmic pathway is involved in developmental onset of ripening in grape berry. *Plant Physiol.* 142: 220–232.